Traffic

Published by John Wiley & Sons Ltd
doi:10.1111/tra.12383

Review

Structural Basis of Cargo Recognition by Unconventional Myosins in Cellular Trafficking

Jianchao Li[1], Qing Lu[1] and Mingjie Zhang[1,2,*]

[1]Division of Life Science, State Key Laboratory of Molecular Neuroscience, Hong Kong University of Science and Technology, Clear Water Bay, Kowloon, Hong Kong, China
[2]Center of Systems Biology and Human Health, School of Science and Institute for Advanced Study, Hong Kong University of Science and Technology, Clear Water Bay, Kowloon, Hong Kong, China
*Corresponding author: Mingjie Zhang, mzhang@ust.hk

Abstract

Unconventional myosins are a superfamily of actin-based molecular motors playing diverse roles including cellular trafficking, mechanical supports, force sensing and transmission, etc. The variable neck and tail domains of unconventional myosins function to bind to specific cargoes including proteins and lipid vesicles and thus are largely responsible for the diverse cellular functions of myosins *in vivo*. In addition, the tail regions, together with their cognate cargoes, can regulate activities of the motor heads. This review outlines the advances made in recent years on cargo recognition and cargo binding-induced regulation of the activity of several unconventional myosins including myosin-I, V, VI and X in cellular trafficking. We approach this topic by describing a series of high-resolution structures of the neck and tail domains of these unconventional myosins either alone or in complex with their specific cargoes, and by discussing potential implications of these structural studies on cellular trafficking of these myosin motors.

Keywords cargo recognition, cargo transport, myosin tail domain, myosin-I, myosin-V, myosin-VI, myosin-X, unconventional myosins

Received 2 December 2015, revised and accepted for publication 29 January 2016, uncorrected manuscript published online 4 February 2016

Molecular motors are a set of biological nano-scale engines that can efficiently convert chemical energy into mechanical work via hydrolysis of nucleotide triphosphates such as ATP or GTP. Molecular motors operating in living organisms include, but are not limited to, the following several classes: cytoskeletal motors (e.g. myosin, dynein and kinesin), rotary motors (e.g. F_oF_1-ATP synthase), polymerization motors (e.g. actin and dynamin) and nucleic acid motors (e.g. RNA/DNA polymerase) (1). Among the three major families of cytoskeletal motors, dyneins and kinesins are microtubule-based motors, and myosins are actin filament-based motors (2).

Myosins are widely expressed in all eukaryotic species, and can be classified into more than 20 different classes (3). Human genome contains about 40 different myosin genes, which can be grouped into 12 subfamilies (Figure 1). Overall, myosins are divided into two major groups, namely conventional myosin-II and unconventional myosins (4). Conventional myosin-II, expressed in muscle cells and in contractile rings of non-muscle cells, contains a long coiled coil dimerization domain at their C-termini and forms bipolar filaments (5,6). The rest of myosin motors are collectively called unconventional myosins, and they are very divergent in the regions outside their motor domains and correspondingly play extremely diverse cellular functions (7,8).

One of the major functions of unconventional myosins is vesicle trafficking such as intracellular vesicular transport, endocytosis and exocytosis (9). For example, myosin-V, a plus-end-directed motor, is responsible for

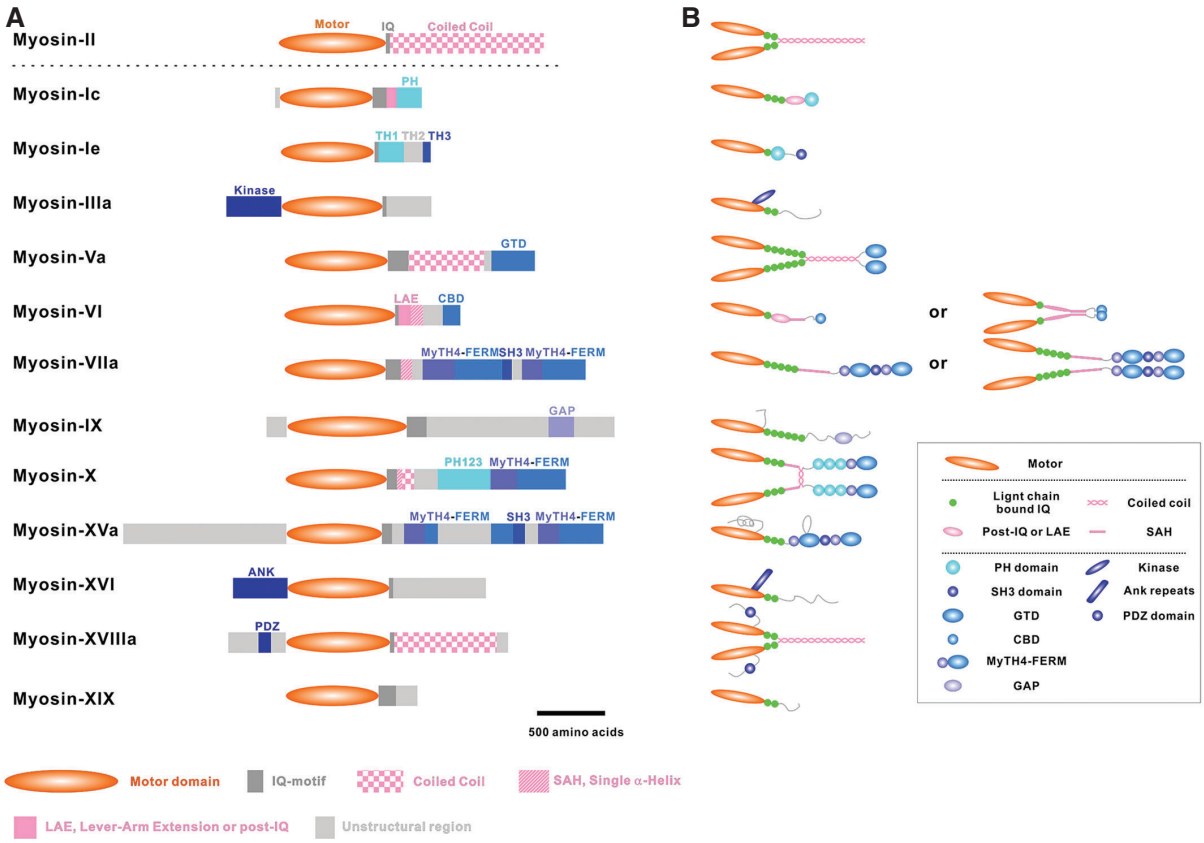

Figure 1: Schematic representations showing the overall architectures of human myosins. A) All the myosins have conserved motor heads (orange), different numbers of IQ motifs (gray) followed by a helical region (pink) and distinct tails with various functional domains. B) Schematic representations of myosin structures. Myosin-II, -Va, -X and -XVIII exist as constitutive dimers and myosin-VI and myosin-VIIa may exist in both monomeric and dimeric forms.

transporting many exocytic vesicles toward plasma membranes (10). In contrast, the minus-end-directed myosin motor, myosin-VI, transports endocytic vesicles toward cell interiors (11,12). Myosin-I, a class of single-headed myosin motors, have also been shown to participate in exocytosis, endocytosis and *trans*-Golgi network trafficking by tethering vesicles to the cortical actin filaments (13). In this review, we focus on the structural basis of cargo recognition and cargo binding-induced changes in the activity of unconventional myosins. To fit with the scope of this thematic issue, we will further limit our discussions on the roles of unconventional myosins in cellular trafficking processes. We will start by giving an overview of the general architectures of unconventional myosins, and then provide several examples of how individual myosins coordinate with their cargoes to fulfill their cellular trafficking roles.

Overall Architectures of Unconventional Myosins

Each myosin contains a characteristic 80-kDa motor domain usually located at the very N-terminal end (Figure 1). The motor domain can hydrolyze ATP as well as directly bind to actin filaments. The ATPase cycle is coupled to conformational changes and actin-binding capability of the motor domain (5,14,15). During each ATPase cycle, the amount of time a motor spends tightly bound to F-actin (a parameter known as the duty ratio) is different for different myosin motors, and this is intimately linked to the specific functions of each myosin (16–18). The duty ratio for conventional myosin-II is around 0.05. This low duty ratio ensures the high sliding speed of polymerized myosin-II on actin filaments (5,19,20). The duty ratios for some of the unconventional myosins

(e.g. myosin-V and myosin-VI) are much higher than that of myosin-II. The high duty ratios of these unconventional myosins are matched with the processive movements of these myosins along actin filaments during cargo transportation (18). Myosin-I family motors are very unique as their duty ratios can dramatically change from a very high value to a very low one (e.g. from >0.9 to <0.2 for myosin-Ib) when load applied to the motor tail is removed (13,21,22). The load-dependent duty ratio changes may be correlated with the Ca^{2+}-induced cargo unloading events of myosin-I (23). We will not go into further details here, and readers are referred to several excellent reviews on this topic (5,14,15).

Following the motor head, each myosin invariably contains a neck region composed of various numbers of continuous IQ motifs (isoleucine-glutamine motifs) (Figure 1). The IQ motifs can form a continuous and stable α-helix upon Calmodulin (CaM) or CaM-like light chain binding, thus acting as a lever arm to amplify the motion induced by the conformational change of the motor domain during each ATPase cycle (24). The number of IQ motifs is directly correlated with the step sizes of unconventional myosins on actin filaments (25). In the majority of unconventional myosins, the neck region is immediately followed by a helical sequence with variable lengths (segments highlighted in pink in Figure 1). These helical segments can form several distinct types of structures that are uniquely suited for specific functions of each motor. For example, myosin-V contains a very long parallel coiled coil that can dimerize the motor and facilitate its hand-over-hand movement along actin filaments (26–30). Myosin-X also contains a coiled coil domain, but this coiled coil domain forms an anti-parallel dimer instead of a parallel coiled coil dimer. The formation of the anti-parallel coiled coil dimer may facilitate the motor to adopt a straddled walking mode on bundled actin filaments (31,32) in addition to the conventional hand-over-hand walking mode on single actin filament (33,34). However, whether the proposed straddled walking mode is indeed adopted by the full-length myosin-X remains to be established. Several myosins (e.g. myosin-VI/VII/X) contain a highly charged and very stable single α-helix (SAH) with various lengths after their neck region (Figure 1). These rigid SAHs can extend the lengths of the lever arms and thereby modulate the step sizes of these motors (35,36). Myosin-VI contains a ~80-aa helical region known as lever arm extension (LAE). It folds into a three-helix bundle (~3 nm in length) in the absence of cargo binding but extends into a semi-rigid, elongated helix 6–9 nm in length upon cargo binding (37,38). This cargo binding-induced LAE contributes to the very large step size (~36 nm) of myosin-VI (37,38). Myosin-Ic, and likely other short-tailed myosin-Is including myosin-Ia, Ib, Id, Ig and Ih, contain an atypical helical domain (known as the post-IQ region, see below for details) following the canonical IQ motifs. The post-IQ domain of myosin-Ic forms a three-helix bundle and binds to apo-CaM with a mode that is totally different from all other known CaM/target interactions. Importantly, the conformation of the myosin-Ic post-IQ/CaM complex becomes flexible upon Ca^{2+} concentration increase, presumably leading to a decrease in load and subsequent detachment of the motor from actin filaments (23).

The tails of unconventional myosins are highly variable (Figure 1) and presumably dictate the cargo recognition specificities of the myosins (7,39,40). Several myosins contain well-characterized protein–protein or protein–lipid interacting domains such as SH3 (Src homology 3) domain in myosin-I/VII/XV, ankyrin repeats in myosin-XVI, PDZ (PSD95/Dlg/ZO1) domain in myosin-XVIII and PH (pleckstrin homology) domain in myosin-I/X. It is noted that the PDZ domain of myosin-XVIII and the ankyrin repeats in myosin-XVI are situated at the very N-terminal ends and proceed the motor heads in their primary sequences. Topologically, the N-terminus of the motor domain is at the opposite side of the actin-binding site of the motor head; thus, the PDZ domain and the ankyrin repeats located at the N-terminal ends will not interfere with actin binding to the motor domains and can also be regarded as cargo-binding domains (CBDs) of these two motors. Several myosins contain well-folded domains that are specific to myosin motors. These myosin-specific, cargo recognition domains include the MyTH4-FERM (myosin tail homology 4, band 4.1/Ezrin/Radixin/Moesin) tandems in myosin-VII/X/XV, CBD in myosin-VI and globular tail domain (GTD) in myosin-V. Interestingly, two unconventional myosins (myosin-III/IX) contain domains with enzymatic activities, and these two myosins can be regarded as motorized signaling molecules (41). The kinase domain located at the N-terminus of myosin-III has been shown to regulate the ATPase activity by direct

phosphorylation of the motor domain (42,43). The RhoGAP domain at the tail of myosin-IX has been implicated in regulating RhoA GTPase activity, thereby modulating the actin cytoskeletal dynamics (44–46).

Cargo-Mediated Dimerization of Myosin-VI

Several myosins including myosin-VI/VII are known to function both as actin filament-based transporters and as mechano-tethers between cell cortex and actin filaments (7,40,47). Intuitively, dimerization of myosins can promote their processive movements along actin filaments, and a monomeric myosin would be better suited to function as a mechano-tether. It is noted that neither myosin-VI nor myosin-VII contains a well-defined coiled coil dimerization domain (Figure 1), suggesting that, in contrast to myosin-V, myosin-VI/VII do not form a constitutive dimer on their own (35,36,48). This analysis raises a possibility that cargoes with specific cellular functions may dictate the corresponding functions of certain myosins. For example, cargoes located on transporting vesicles may somehow be able to convert myosins into processive transporters, and certain cargoes located on the cell cortex that function as mechanical anchors may 'instruct' myosins to adopt a monomer conformation. One such example is myosin-VI (49–53), the only known myosin that travels toward the minus-end of actin filaments (54,55). The atomic structure of myosin-VI shows that in the absence of its cargo adaptor disabled homologue 2 (Dab2), the CBD of myosin-VI exists as a stable monomer (Figure 2A). Binding of myosin-VI-interacting region (MIR) of Dab2 facilitates the formation of 2:2 myosin-VI CBD/Dab2 MIR complex. The crystal structure shows that, in the symmetric 2:2 complex, the N- and C-terminal helices from the two Dab2 molecules bind to the opposite sides of CBD (Figure 2B). There are very little contacts in the interface between the two CBDs, suggesting that the dimer formation will only occur when Dab2 MIR binds. The binding of Dab2 to myosin-VI can convert myosin-VI from a non-processive monomer to a processive dimer (50,52). The interactions between Dab2 and transmembrane proteins such as the low-density lipoprotein receptor on endocytic vesicles (56) link myosin-VI to clathrin-coated endocytic vesicles (Figure 2C). Besides the dimerization induced by monomeric cargo adaptor Dab2, it has also been suggested that dimerization of myosin-VI can also be triggered by intrinsically homodimeric cargo adaptor optineurin (51,57). Such cargo binding-induced functional change of myosin-VI is further manifested by the conformational changes in its LAE region. Experiments using both fragments containing the LAE region and much longer versions of myosin-VI suggested that binding of cargo vesicles can trigger extension of myosin-VI LAE from a three-helix bundle to an extended, semi-rigid SAH (37,38), which can be further stabilized by Ca^{2+}-CaM (58,59). As such, a trafficking cargo-bound form of myosin-VI forms a transport–competent dimer with an extended lever arm capable of taking ~36 nm steps walking along actin filaments (37,38,60).

It should also be noted that there are several other cargoes such as LMTK2 (Lemur tyrosine kinase 2) and GIPC (GAIP C-terminus-interacting protein) (61,62), which are not known to dimerize myosin-VI. With these cargoes loaded, myosin-VI may still exist as a monomer, and these myosin-VI/cargo interactions may play certain tethering roles instead of actin filament-based transportation. Alternatively, additional mechanisms (e.g. simultaneous binding of two or more cargo proteins to CBD and its preceding ~90-residue subdomain) may exist to turn myosin-VI into a processive dimer for transport.

The cargo-induced dimerization mechanism has also been observed in several other myosins, such as myosin-VIIa and yeast Myo4p. Myosin-VIIa also exists as a monomer before binding to cargoes, but has been implicated to turn into a transport–competent dimer upon binding to its cargo complex Myrip/Rab27a (63). Unlike its mammalian myosin-V orthologs, yeast Myo4p is intrinsically monomeric (64). It has been suggested that binding to a coiled coil cargo adaptor She3p via its GTD can convert Myo4p into a dimer, and facilitate Myo4p-mediated transport of messenger ribonucleoprotein particles (65). Inspecting the domain organization of the myosins shown in Figure 1 reveals that several additional myosins lack obvious coiled coil dimerization domains. It remains to be tested whether these myosins may also adopt cargo-induced dimerization to regulate their actin filament-based transport functions.

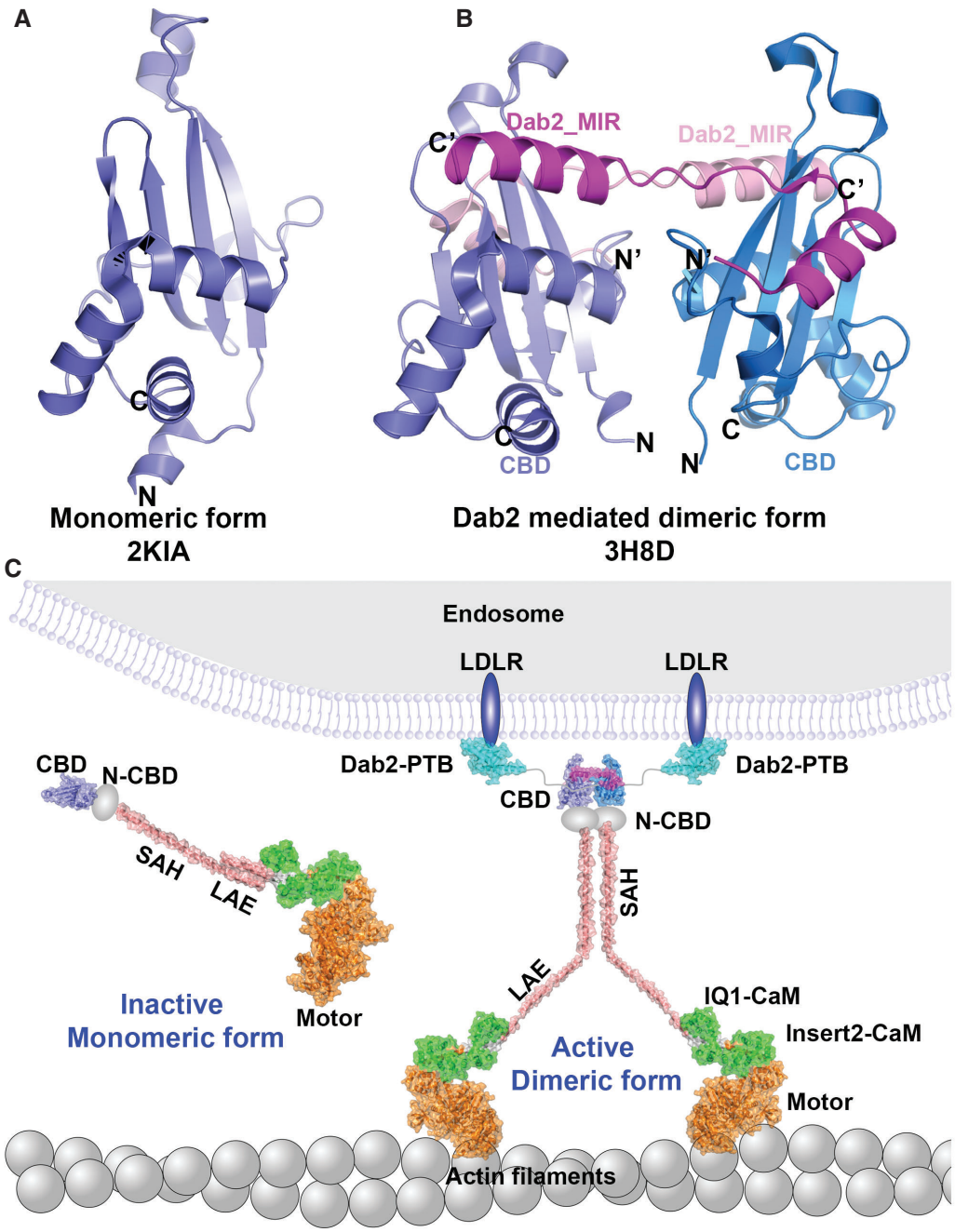

Figure 2: Cargo-induced dimerization of myosin-VI. A) The NMR (nuclear magnetic resonance) structure of the monomeric, apo-form myosin-VI CBD (PDB (protein data bank) code: 2KIA). B) Binding of cargo adaptor Dab2 MIR induces the CBD to form a 2:2 complex (PDB code: 3H8D). C) A walking model depicting myosin-VI with the dimerized tails induced by cargo adaptor binding and membrane-induced LAE expansion in endosome trafficking. In the absence of cargo loading, myosin-VI adopts an inactive, monomeric conformation (left). Dimerization induced by Dab2 binding can facilitate the actin filament-based endosome trafficking (right) both by inducing myosin-VI dimer formation and by tethering vesicles with the dimerized motor. In this image, the extended LAE is modeled by fusing the three helices into a continuous one and the SAH was modeled as an ideal SAH.

Cargo Binding and Cargo-Mediated Release of Myosin-V Auto-Inhibition

The activity of myosins, similar to all other enzymes, is subject to fine regulatory controls in order to prevent futile hydrolysis of ATP. A common strategy used by myosins is to keep motors in their auto-inhibited conformation before engaging their cargoes (66–72). One of the best-studied auto-inhibitory myosin regulatory systems is in myosin-Va (Figure 3). It has been shown that the full-length myosin-Va has a low actin-activated ATPase activity in low Ca^{2+} concentration buffer (69). Truncation of the tail or elevating Ca^{2+} concentration will greatly increase its ATPase activity (67,68). Electron microscopic (EM) studies revealed that the full-length myosin-Va adopts a folded dimeric structure, with its GTD folding back to bind to the motor domain (Figure 3A) (27,28). Charge–charge interactions play a critical role in the auto-inhibition of myosin-Va, as simply increasing the buffer salt concentration can induce conformational changes and activate the ATPase activity of the motor (67,68). Based on the available crystal structures of the motor head combined with mutagenesis studies, the auto-inhibition of myosin-Va was deduced to be mediated between a few positively charged residues from GTD subdomain II and several negatively charged residues from the N-terminal subdomain of the motor domain (28,73,74).

As the auto-inhibition involves GTD, it has been proposed that cargo binding can release the auto-inhibition of myosin-Va (75). Melanophilin (Mlph) is probably the best-studied cargo protein of myosin-Va (Figure 3B). Mlph is an adaptor protein capable of binding to melanosome through binding to small GTPase Rab27a. Formation of the myosin-Va/Mlph/Rab27a complex facilitates melanosome transport (Figure 3C) (76–78). A functional null mutation in myosin-Va blocks this process, thus leading to the 'dilute-lethal' phenotype in rodents (79). Biochemical studies have shown that Mlph can directly stimulate the actin-activated ATPase activity of myosin-Va (75). Furthermore, single molecule experiments also demonstrated that adding Mlph will increase the processivity of the motor (80). However, the Mlph-binding site in GTD is located in subdomain I (73,81), whereas the motor binding site is located in subdomain II (Figure 3A,B). Therefore, the Mlph-mediated activation of myosin-Va is not likely to be caused by direct competition between Mlph and the motor head for GTD. Instead, the binding of Mlph to subdomain I may induce certain conformational changes to the subdomain II of GTD via long-range allosteric couplings, which causes a weakened interaction between the motor head and GTD (82). It should be noted that the Mlph/myosin-Va interaction and Mlph-mediated myosin-Va activation may be more complicated, considering that a melanocyte-specific exon-F, which is located immediately N-terminal to the GTD, is also known to be involved in its binding to Mlph (83). Further work will be required to tease out the detailed molecular mechanism of Mlph-mediated activation of myosin-Va. Similarly, *Drosophila* myosin-V has also been proposed to be auto-inhibited and binding of dRab11 can release the auto-inhibition (84). It will be interesting to test whether binding of Rab11 to vertebrate myosin-Vb will have the same regulatory effect (81). Also, how the activities of myosin-Vc is regulated and what cargo(es) can release its auto-inhibited conformation are unknown.

Auto-inhibition mechanisms have also been reported for other myosins including myosin-Ie (66) and myosin-VIIa (70,71). The recently solved crystal structures of myosin-Ic demonstrated that the entire myosin-Ic adopts a rigid conformation with its C-terminal projecting far away from the motor domain in low Ca^{2+} concentration buffer (23). It is thus unlikely that tail-mediated auto-inhibition would happen for the short-tailed myosin-I. Nonetheless, it is possible that auto-inhibition may occur in the long-tailed myosin-I (myosin-Ie and If) as they lack the rigid post-IQ region and contain additional TH2 and SH3 domains that may fold back to interact with their respective motor domains. The auto-inhibition of myosin-VIIa has been confirmed by a negative staining-based EM imaging study and by direct ATPase activity measurements (70,71). Mutagenesis studies also showed that, similar to the case observed in myosin-Va, several positively charged residues in the C-terminal MyTH4-FERM tandem are important for the inhibition (70,85). Given that the motor domains are quite conserved across different classes of unconventional myosins (86), it is tempting to speculate that the site corresponding to the negatively charged residues identified in myosin-Va head may function as a common auto-inhibitory site for other members of

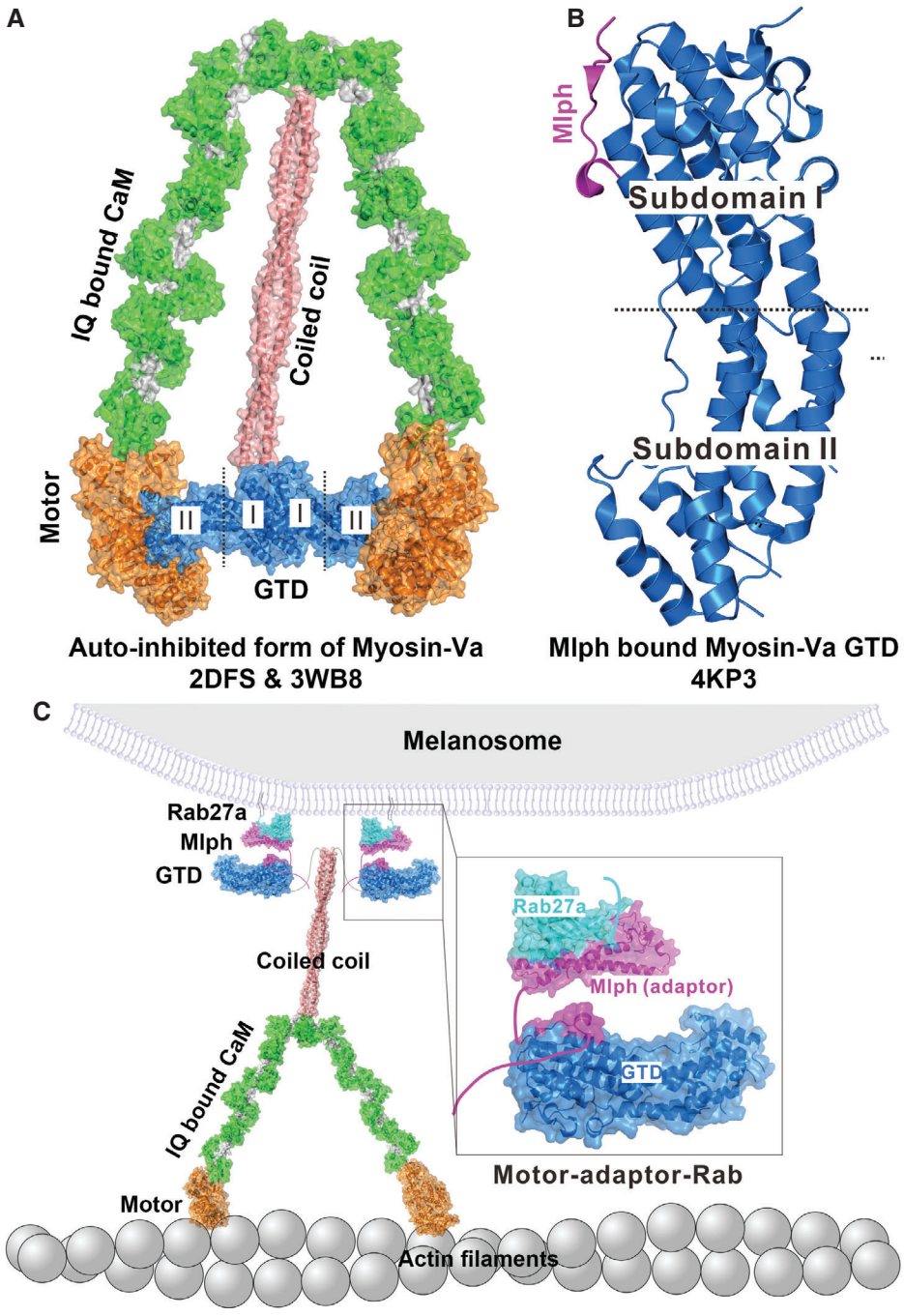

Figure 3: Cargo binding-induced release of myosin-V auto-inhibition. A) Modeled structure of the auto-inhibited conformation of myosin-Va. The model is derived from the auto-inhibited structure (PDB code: 2DFS) and the GTD structure (PDB code: 3WB8) of myosin-Va. The interaction between the motor domain and the subdomain II of GTD is modeled based on their charge–charge interactions described earlier (28,74). B) The structure of myosin-Va GTD in complex with Mlph (PDB code: 4KP3) showing that Mlph binds to subdomain I of GTD. C) A walking model of the open form of myosin-Va in melanosome transportation. The enlarged insert shows that GTD connects with the small GTPase Rab27a using Mlph as the adaptor.

myosins. Obviously, this will need to be tested in future experiments.

Myosin-V Can Specifically Recognize Active Form of Vesicle-Anchored Small GTPase

In addition to binding to Rab effectors, myosin-V can also directly interact with the active form of Rab. Biochemical and structural studies have shown that myosin-Vb can specifically bind to the GTP-bound form of Rab11 (Figure 4A) (81). Binding of Rab11 will directly link the motor to recycling endosomes (Figure 4B), thus facilitating their transportation toward dendritic shafts in neuronal synapses (10). The crystal structures of myosin-Vb GTD in complex with both GTP- and GDP-bound forms of Rab11 explain the difference in their binding affinities (dissociation constants of 0.6 μM for GTP-Rab11 versus 19 μM for GDP-Rab11). The γ-phosphate of GTP stabilizes the conformation of the switch II region of Rab11, which makes direct contacts with myosin-Vb GTD (highlighted in magenta in Figure 4A). The interaction between the Rab11 switch II and myosin-Vb GTD generates additional 400 $Å^2$ contact surface of the complex, and thus enhances its binding to myosin-Vb by ~30-fold (81). Interestingly, in addition to binding to Rab11, it has been reported that myosin-Vb can also bind to the Rab11 adaptor Rab11-FIP2 (87). The simultaneous binding of myosin-Vb to both Rab11-FIP2 and Rab11 can be regarded as a coincident cargo detection mechanism that can provide very high binding affinity as well as specificity between the motor and its cognate cargo vesicle.

The association between myosins and small GTPases has been recognized for a long time. Myosin-Ic has been reported to interact with Ras-related protein A (RalA) for Glut4-containing vesicle exocytosis (88). The motorized signaling molecule myosin-IX contains a GAP domain and can catalyze GTP hydrolysis of RhoA (44,45). The recently determined crystal structure of the myosin-IXb GAP domain elucidated the specific recognition mechanism for RhoA (46). The specific pairings with small GTPases not only determine cargo vesicle binding specificities of unconventional myosins, but also provide possible means for GTPase-dependent cargo vesicle loading/unloading of the motors.

Myosin-X Can Synergistically Bind to Phospholipids and Protein Cargoes

Several unconventional myosins contain multiple functional domains in their tails (Figure 1), suggesting that these motors can engage several different targets simultaneously. For example, the tail of myosin-VIIa consists of two MyTH4-FERM tandems separated by an SH3 domain. The N-terminal MyTH4-FERM tandem of myosin-VIIa forms a stable complex with an adaptor protein SANS as a part of the upper tip link density in the hair cell stereocilia (89–91). The C-terminal MyTH4-FERM tandem of myosin-VIIa has been reported to bind to junctional proteins Vezatin or Shroom2 for its function at cell–cell contacts (92,93). The SH3 domain of myosin-VIIa has been reported to bind to PCDH15, which is a tip-link component of stereocilia (94).

Myosin-X, which evolved after myosin-VIIa (3), also contains a protein-binding MyTH4-FERM tandem in its tail region. Preceeding the MyTH4-FERM tandem of myosin-X are three lipid membrane-binding PH domains (Figure 1). Myosin-X can undergo fast, intra-filopodia movements and is critical for the formation of filopodial structures in various tissues including growth cones of axons and blood vessels (95,96). The three consecutive PH domains and the MyTH4-FERM tandem of myosin-X bind to their respective targets in unique manners. The first PH domain of myosin-X is split into two halves by the second PH domain, and the $PH1_N$-PH2-$PH1_C$ tandem folds together into an integral structural supramodule, in which the two lipid-binding pockets are juxtaposed to each other at the same face of the molecule (Figure 5A) (97). The PH2 domain can specifically bind to $PI(3-5)P_3$, while PH1 and PH3 can non-specifically bind to negatively charged phosphor-lipid membranes (97). The PH123 together can specifically bind to $PI(3,4,5)P_3$-enriched membranes cooperatively and with a high affinity. The PH123 tandem was proposed to function as an acute sensor in detecting PI_3-kinase activations in cellular settings (97). The structure of myosin-X MyTH4-FERM tandem in complex with the cytoplasmic tail of the axon guidance receptor DCC (deleted in colorectal cancer) reveals another protein target-binding mode for myosin MyTH4-FERM tandems (98,99). In this case, a short cytoplasmic tail of DCC binds to the F3 lobe of the FERM domain in the MyTH4-FERM

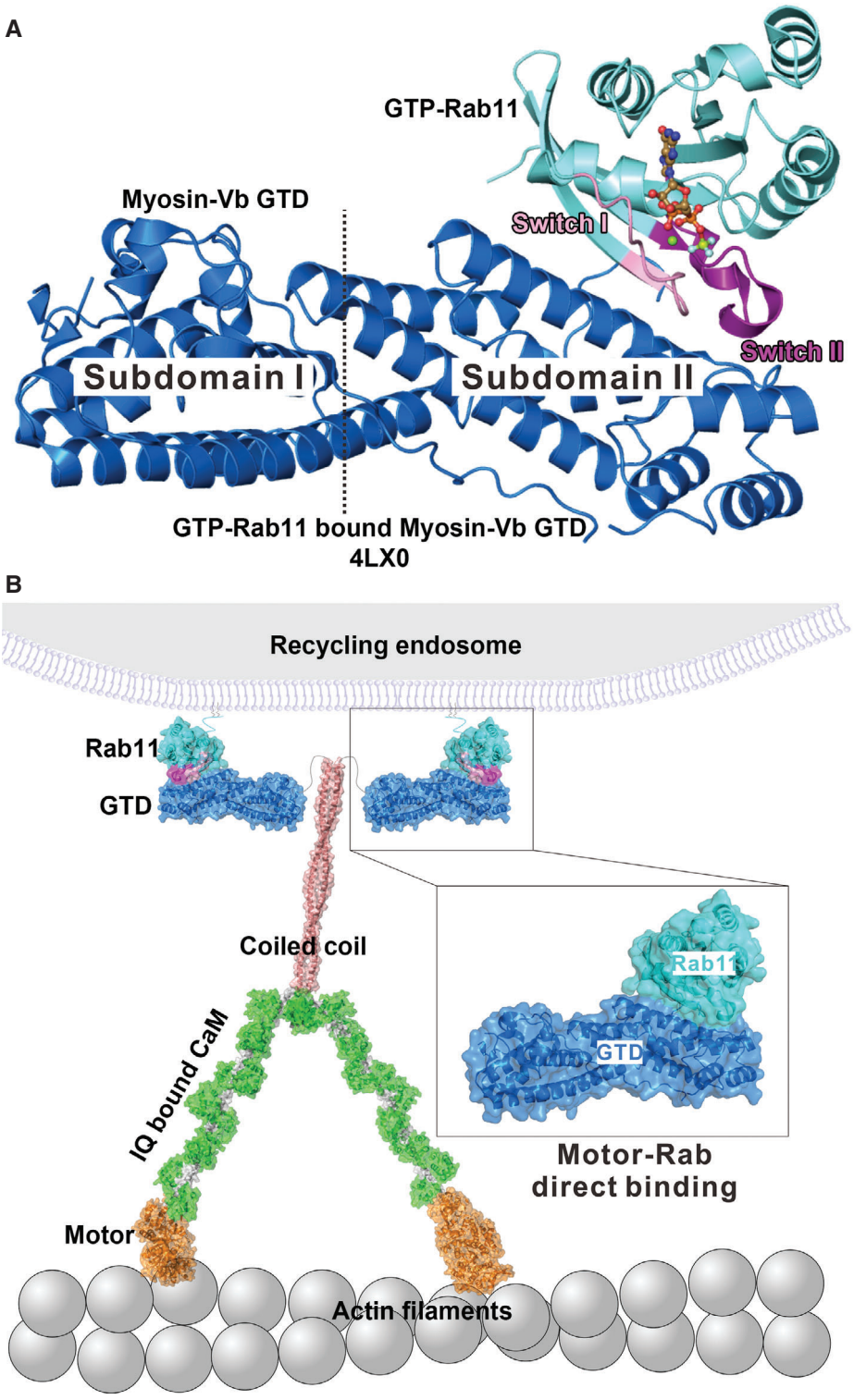

Figure 4: Myosin-Vb specifically binds to GTP-bound Rab11. A) Ribbon diagram of myosin-Vb GTD in complex with GTP-bound Rab11 (PDB code: 4LX0). GTP is highlighted with the stick model. Switch I and II are highlighted in pink and magenta, respectively. B) A walking model of myosin-Vb in the recycling endosome trafficking pathway directly associated with Rab11. The enlarged insert shows the interaction between GTD and Rab11.

supramodule (Figure 5B). As the MyTH4-FERM tandem and the PH123 tandem are arranged immediately next to each other, these two structural components of myosin-X are likely to cooperate with each other to simultaneously recognize the tail of DCC located at the cytoplasmic face of plasma membranes and PI(3–5)P_3 in the inner leaflet of the membranes, respectively (Figure 5C). The cooperative interactions of the PH123 and MyTH4-FERM tandems in the motor tail domain with PI(3,4,5)P_3 and DCC on plasma membranes, respectively, may enable myosin-X to bind to its cargoes with high affinity, exquisite specificity, and at specific cellular regions (e.g. filopodial tips). A potential advantage of such coincident detection is that either one or combination of the two elements can differentially tune the motor cargo interaction. For example, PI_3-Kinase activation will affect membrane association of myosin-X mediated by PH123, and a netrin signal can also impact the motor's membrane binding via its MyTH4-FERM/DCC interaction. Such multidomain cooperation may allow myosin-X to interpret and integrate various cellular signals at filopodia tips, and thereby regulate its cargo transportation specificity.

Ca^{2+}-Dependent Conformational Cycling of Myosin-Ic

In addition to cargo loading-induced activity changes, myosins are also regulated by a class of their intimate binding partners, myosin light chains. Myosin light chains usually interact with and stabilize the IQ motifs in myosins' neck region (100,101). Conventional myosins associate with two functionally different light chains, IQ1 binding to the essential light chain (ELC) and IQ2 binding to the regulatory light chain (RLC). The light chains for unconventional myosins are more diverse, and include CaM, RLC, ELC and some unusual ones like calcium-binding protein 1 (CaBP1), calcium and integrin-binding protein 1 (CIB1), androcam and calmodulin-like protein 3 (CALML3), etc (102); although CaM is regarded as the most prevalent light chain. These light chains share similar structures using EF-hand calcium-binding motifs as their basic building blocks, but can respond to different Ca^{2+} concentration fluctuations. Ca^{2+}-mediated dissociations/associations of light chains from the myosin heavy chains often directly regulate the ATPase activities of the motor domains or cargo-binding capabilities of unconventional myosins. The exact combinations of light chains used by each unconventional myosin under physiological conditions are likely to be very complicated, and little is known at the current stage (102).

An intriguing example of Ca^{2+}-mediated conformational regulation of myosin by its light chains is myosin-Ic (23,103–106). Piecing together the crystal structures of the motor domain and the neck and tail domain of myosin-Ic reveals that the full-length myosin-Ic adopts a rigid conformation with three stably associated apo-CaM under low Ca^{2+} concentration (Figure 6A) (23,106). A myosin-Ic-specific insertion within the motor domain makes additional contact with the IQ1-bound CaM (106), which may be the underlying mechanistic basis for the direct communication between Ca^{2+} binding to the light chain and the ATPase cycle of the motor domain. Direct contact between the motor domain and CaM bound to IQ1 has also been observed in myosin-Ib, in which an N-terminal region of the motor domain contacts with IQ1-bound CaM (107). In its neck and tail domain, myosin-Ic contains a previous unrecognized post-IQ region. This post-IQ region, together with IQ3, binds to apo-CaM using a mechanism that has never before been observed for any EF-hand CaBPs (23). In this interaction, the two helices of first EF-hand of the N-lobe of CaM are completely uncoupled, and form a compact, helical bundle structure with the three α-helices of the myosin-Ic post-IQ. The post-IQ/CaM structural unit interacts with the neck domain on one side and couples with the C-terminal extended, lipid membrane-binding PH domain on the other side, forming a rigid neck-tail region of myosin-Ic (Figure 6A). The rigid conformation of myosin-Ic, with its motor head engaging actin filaments and its tail extended PH domain attaching plasma membranes, is ideally suited for mechanical force transmission between actin cytoskeletons and cell cortices (Figure 6B, left). The rigid conformation of myosin-Ic is likely to be important for the motor to tether exocytic/endocytic vesicles to membranes prior to the fusion events, and to maintain cell–cell junctions with mechanical strains (Figure 6C,D). Importantly, upon Ca^{2+} concentration increases, myosin-Ic undergoes substantial conformational changes. The rearrangement of CaM binding will cause part of the neck and post-IQ region to become unstructured, thus increasing

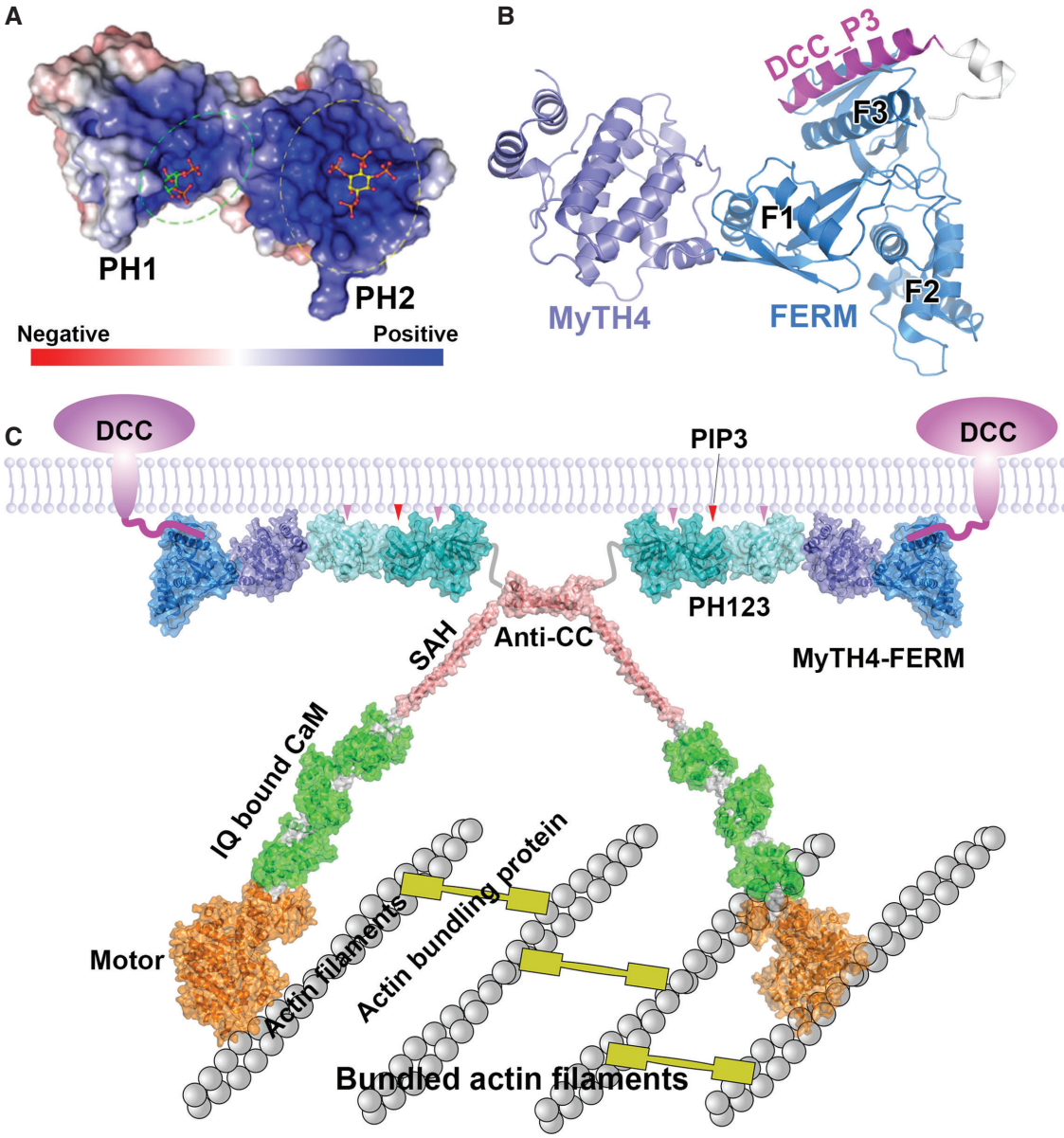

Figure 5: Multidomain cooperation of the myosin-X tail. A) Electrostatic potential surface of the $PH1_N$-PH2-$PH1_C$ tandem showing the two distinct positively charged lipid-binding pockets rendering the PH tandem as a high-affinity, cooperative $PI(3-5)P_3$ sensor. The $Ins(1,4,5)P_3$ and $Ins(1,3,4,5)P_4$ (shown in the stick models) are modeled into the lipid-binding pockets of PH1 and PH2, respectively, as described earlier (97). B) Ribbon representation of the MyTH4-FERM/DCC_P3 complex structure showing the specific DCC binding of myosin-X. C) Structural model of the full-length, dimeric myosin-X simultaneously bound to DCC and $PI(3,4,5)P_3$-containing membranes via its tail domains. The model also illustrates that the anti-parallel coiled coil dimerized myosin-X may walk on bundled actin filaments with a straddled walking mode. The structure of the motor domain is a homologous model using the structure of myosin subfragment-1 (PDB code: 2MYS) as the template; the IQ-CaM complex is also a homologous model using the structure of myosin-V IQ1-CaM complex (PDB code: 2IX7) as the template; the SAH was modeled as an ideal α-helix and the PH3 domain is a homology model using the myosin-X PH2 domain (PDB code: 3TFM) as the template.

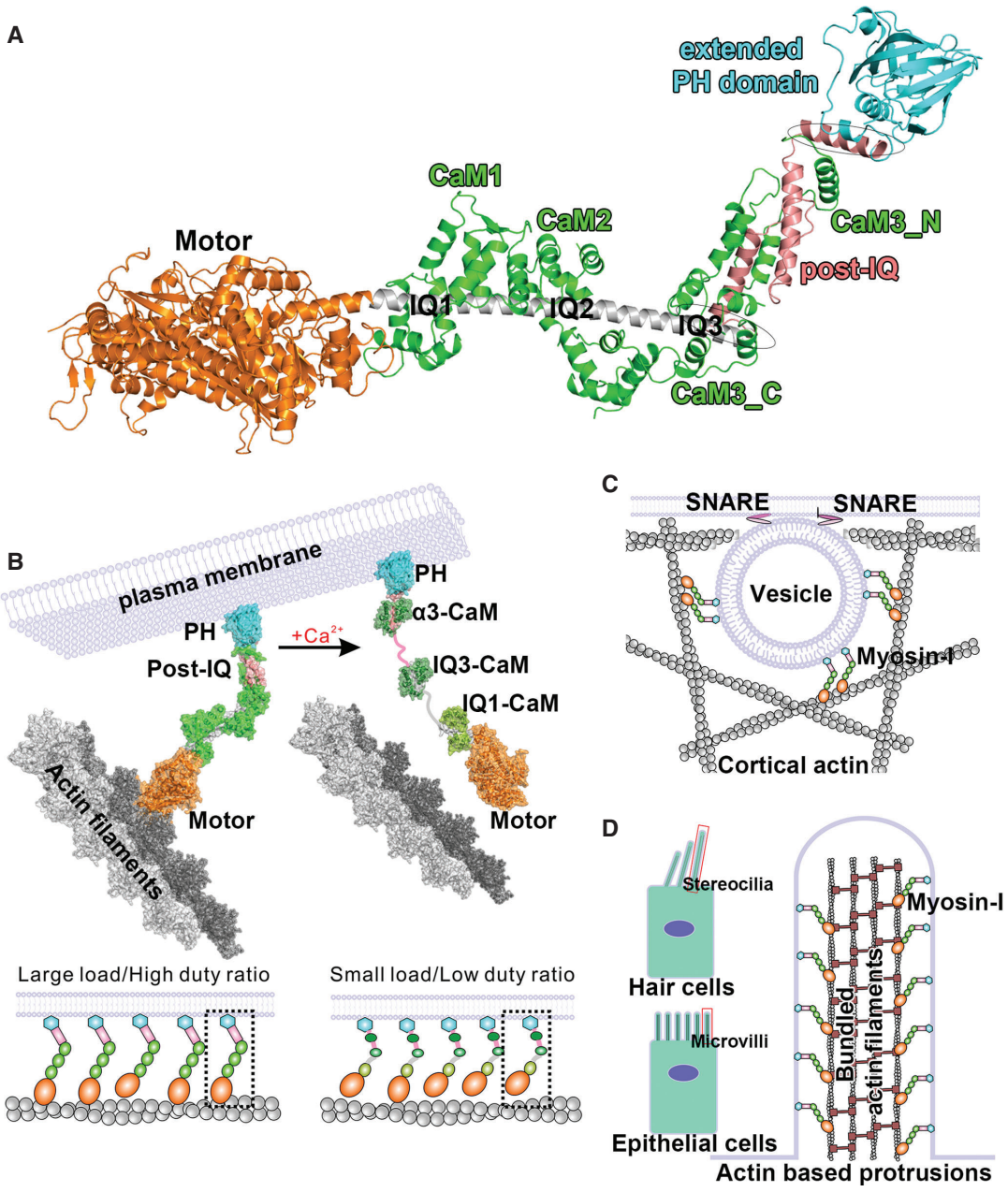

Figure 6: Myosin-Ic undergoes Ca^{2+}-dependent cycling of rigid and flexible conformational states. A) Ribbon diagram of a modeled full-length myosin-Ic structure in complex with three copies of CaM under low Ca^{2+} concentration. The generation of the full-length myosin-Ic structure was described earlier using a combination of the structure of the myosin-Ib motor domain (PDB code: 4L79) and the structure of myosin-Ic neck-tail domain (PDB code: 4R8G) (23). B) A model of the full-length myosin-Ic structure shows the rigid conformation of myosin-Ic under low Ca^{2+} concentration (left). The rigid conformation is suitable for mechanical force transmission between actin cytoskeletons and cell cortices. Binding of Ca^{2+} to CaM converts myosin-Ic from the rigid conformation to a more flexible conformation, leading to dissipation of loads, which will further promote the dissociation of the motor head from the actin filaments (right). C) Schematic models showing that class I myosins are involved in tethering exocytic vesicles between actin filaments and plasma membranes before final fusion events. D) Schematic models showing how class I myosins may function to maintain tension in cellular protrusions such as stereocilia and microvilli.

the flexibility of its neck-tail region. The Ca^{2+}-induced loss of structural rigidity is accompanied by dissipation of force experienced by the myosin-Ic tail and consequent lowering of the mechanical load of the motor. The decrease of the mechanical load leads to a lower duty ratio, which further promotes detachments of myosin-Ic from actin filaments (Figure 6B, right). When cells return to the resting state, lowering of Ca^{2+} concentration allows the rapid re-binding of apo-CaM to the neck tail region and recovery of the conformational rigidity of myosin-Ic, as several CaM molecules remain bound to myosin-Ic even at high Ca^{2+} concentrations (23). Based on their sequence conservation, we believe that the Ca^{2+}-dependent conformational cycling observed in myosin-Ic is a common property of the short-tailed myosin-I subfamily. It has been implicated that the long-tailed myosin-Is lacking the post-IQ region may also be regulated by Ca^{2+} binding to its light chains (66), but the detail mechanism has not yet been determined

Other unconventional myosins such as myosin-V can also be regulated by their light chains. As discussed previously, myosin-V adopts an auto-inhibited conformation and besides cargo binding, Ca^{2+} concentration elevation can also release the auto-inhibition (67–69). It has been suggested that Ca^{2+} binding to IQ1-bound CaM will induce a conformational change in the motor-IQ1 fragment and thus release the auto-inhibition by its GTD (108). However, the detailed mechanism of the Ca^{2+}-induced auto-inhibition release in myosin V awaits further investigation.

Conclusion and Perspectives

In the past two decades, structural biology has greatly advanced our knowledge about many aspects of the unconventional myosins, such as the catalytic cycles of their motor heads, dimerization modes necessary for their processive movements, cargo recognition mechanisms for binding to specific cargoes and Ca^{2+}-regulated light chain binding and modulations of motor structure and functions.

Despite these great advances, many outstanding questions remain to be answered. First of all, although auto-inhibition has been observed for several myosins and is regarded as a general property for the majority, if not all myosins, the lack of atomic-resolution structures of any of the auto-inhibited myosins has prevented us from a detailed understanding of their auto-inhibitory and corresponding activation mechanisms. Moreover, regulation of cargo loading/unloading of myosins has always been a fascinating question, as myosin-mediated cellular trafficking and other events should be precisely controlled processes in living organisms. Again very little is known in this regard. Although this review briefly discusses small GTPase activity-dependent cargo binding and lipid signaling, it is very likely that other regulatory means such as posttranslation modifications, cargo degradations, metal ion-dependent cargo loading/unloading and alternative splicings of both motor and cargoes are also adopted to control myosin/cargo interactions (7). Elucidating such regulatory mechanisms will be important for understanding the cellular functions of unconventional myosins. Furthermore, several myosins, via their tail regions, can directly bind to actin cytoskeletal regulatory proteins (e.g. myosin-IIIa/b bind to espin-1, myosin-XVa binds to Eps8 and myosin-VIIa binds to Twinfilin-2) (109–112). It is possible that these myosins may directly regulate the actin filament/bundle structures and dynamics in actin-based cellular protrusions such as microvilli and stereocilia (113). Finally, recent major advances in the high-resolution cryo-EM imaging technology, together with other biophysical techniques such as single molecule biophysics, super-resolution imaging and conventional structural biology techniques, will undoubtedly offer wonderful opportunities to elucidate the functional mechanisms of unconventional myosins at an unprecedented level in the next few years.

Acknowledgments

Research in M. Z.'s lab has been supported by grants from the Research Grants Council of Hong Kong (663812, 664113 and AoE/M09/12) and a 973 Program Grant from the Ministry of Science and Technology of the People's Republic of China (2014CB910201). We apologize to colleagues for not being able to cite their work relevant to this review due to the space limitations.

References

1. Vale RD. Millennial musings on molecular motors. Trends Cell Biol 1999;9:M38–M42.
2. Vale RD. The molecular motor toolbox for intracellular transport. Cell 2003;112:467–480.

3. Foth BJ, Goedecke MC, Soldati D. New insights into myosin evolution and classification. Proc Natl Acad Sci USA 2006;103:3681–3686.
4. Berg JS, Powell BC, Cheney RE. A millennial myosin census. Mol Biol Cell 2001;12:780–794.
5. Geeves MA, Holmes KC. Structural mechanism of muscle contraction. Annu Rev Biochem 1999;68:687–728.
6. Beach JR, Hammer JA III. Myosin II isoform co-assembly and differential regulation in mammalian systems. Exp Cell Res 2015;334:2–9.
7. Hartman MA, Finan D, Sivaramakrishnan S, Spudich JA. Principles of unconventional myosin function and targeting. Annu Rev Cell Dev Biol 2011;27:133–155.
8. Hartman MA, Spudich JA. The myosin superfamily at a glance. J Cell Sci 2012;125(Pt 7):1627–1632.
9. Akhmanova A, Hammer JA III. Linking molecular motors to membrane cargo. Curr Opin Cell Biol 2010;22:479–487.
10. Hammer JA III, Sellers JR. Walking to work: roles for class V myosins as cargo transporters. Nat Rev Mol Cell Biol 2012;13:13–26.
11. Buss F, Spudich G, Kendrick-Jones J. Myosin VI: cellular functions and motor properties. Annu Rev Cell Dev Biol 2004;20:649–676.
12. Tumbarello DA, Kendrick-Jones J, Buss F. Myosin VI and its cargo adaptors – linking endocytosis and autophagy. J Cell Sci 2013;126(Pt 12):2561–2570.
13. McConnell RE, Tyska MJ. Leveraging the membrane – cytoskeleton interface with myosin-1. Trends Cell Biol 2010;20:418–426.
14. Ruppel KM, Spudich JA. Structure-function analysis of the motor domain of myosin. Annu Rev Cell Dev Biol 1996;12:543–573.
15. Sweeney HL, Houdusse A. Structural and functional insights into the myosin motor mechanism. Annu Rev Biophys 2010;39:539–557.
16. De La Cruz EM, Ostap EM. Relating biochemistry and function in the myosin superfamily. Curr Opin Cell Biol 2004;16:61–67.
17. O'Connell CB, Tyska MJ, Mooseker MS. Myosin at work: motor adaptations for a variety of cellular functions. Biochim Biophys Acta 2007;1773:615–630.
18. Bloemink MJ, Geeves MA. Shaking the myosin family tree: biochemical kinetics defines four types of myosin motor. Semin Cell Dev Biol 2011;22:961–967.
19. Howard J. Molecular motors: structural adaptations to cellular functions. Nature 1997;389:561–567.
20. Huxley A. How molecular motors work in muscle. Nature 1998;391:239–240.
21. Laakso JM, Lewis JH, Shuman H, Ostap EM. Myosin I can act as a molecular force sensor. Science 2008;321:133–136.
22. Greenberg MJ, Ostap EM. Regulation and control of myosin-I by the motor and light chain-binding domains. Trends Cell Biol 2013;23: 81–89.
23. Lu Q, Li J, Ye F, Zhang M. Structure of myosin-1c tail bound to calmodulin provides insights into calcium-mediated conformational coupling. Nat Struct Mol Biol 2015;22:81–88.
24. Block SM. Fifty ways to love your lever: myosin motors. Cell 1996;87:151–157.
25. Purcell TJ, Morris C, Spudich JA, Sweeney HL. Role of the lever arm in the processive stepping of myosin V. Proc Natl Acad Sci USA 2002; 99:14159–14164.
26. Cheney RE, O'Shea MK, Heuser JE, Coelho MV, Wolenski JS, Espreafico EM, Forscher P, Larson RE, Mooseker MS. Brain myosin-V is a two-headed unconventional myosin with motor activity. Cell 1993;75:13–23.
27. Liu J, Taylor DW, Krementsova EB, Trybus KM, Taylor KA. Three-dimensional structure of the myosin V inhibited state by cryoelectron tomography. Nature 2006;442:208–211.
28. Thirumurugan K, Sakamoto T, Hammer JA III, Sellers JR, Knight PJ. The cargo-binding domain regulates structure and activity of myosin 5. Nature 2006;442:212–215.
29. Li Y, Brown JH, Reshetnikova L, Blazsek A, Farkas L, Nyitray L, Cohen C. Visualization of an unstable coiled coil from the scallop myosin rod. Nature 2003;424:341–345.
30. Yildiz A, Forkey JN, McKinney SA, Ha T, Goldman YE, Selvin PR. Myosin V walks hand-over-hand: single fluorophore imaging with 1.5-nm localization. Science 2003;300:2061–2065.
31. Nagy S, Ricca BL, Norstrom MF, Courson DS, Brawley CM, Smithback PA, Rock RS. A myosin motor that selects bundled actin for motility. Proc Natl Acad Sci USA 2008;105:9616–9620.
32. Lu Q, Ye F, Wei ZY, Wen ZL, Zhang MJ. Antiparallel coiled-coil-mediated dimerization of myosin X. Proc Natl Acad Sci USA 2012;109:17388–17393.
33. Sun Y, Sato O, Ruhnow F, Arsenault ME, Ikebe M, Goldman YE. Single-molecule stepping and structural dynamics of myosin X. Nat Struct Mol Biol 2010;17:485–491.
34. Takagi Y, Farrow RE, Billington N, Nagy A, Batters C, Yang Y, Sellers JR, Molloy JE. Myosin-10 produces its power-stroke in two phases and moves processively along a single actin filament under low load. Proc Natl Acad Sci USA 2014;111:E1833–E1842.
35. Knight PJ, Thirumurugan K, Xu YH, Wang F, Kalverda AP, Stafford WF, Sellers JR, Peckham M. The predicted coiled-coil domain of myosin 10 forms a novel elongated domain that lengthens the head. J Biol Chem 2005;280:34702–34708.
36. Peckham M. Coiled coils and SAH domains in cytoskeletal molecular motors. Biochem Soc Trans 2011;39:1142–1148.
37. Mukherjea M, Llinas P, Kim H, Travaglia M, Safer D, Menetrey J, Franzini-Armstrong C, Selvin PR, Houdusse A, Sweeney HL. Myosin VI dimerization triggers an unfolding of a three-helix bundle in order to extend its reach. Mol Cell 2009;35:305–315.
38. Yu C, Lou JZ, Wu JJ, Pan LF, Feng W, Zhang MJ. Membrane-induced lever arm expansion allows myosin VI to walk with large and variable step sizes. J Biol Chem 2012;287:35021–35035.
39. Krendel M, Mooseker MS. Myosins: tails (and heads) of functional diversity. Physiology (Bethesda) 2005;20:239–251.
40. Lu Q, Li J, Zhang M. Cargo recognition and cargo-mediated regulation of unconventional myosins. Acc Chem Res 2014;47:3061–3070.
41. Bahler M. Are class III and class IX myosins motorized signalling molecules? Biochim Biophys Acta 2000;1496:52–59.

42. Kambara T, Komaba S, Ikebe M. Human myosin III is a motor having an extremely high affinity for actin. J Biol Chem 2006;281:37291–37301.
43. Dose AC, Ananthanarayanan S, Moore JE, Burnside B, Yengo CM. Kinetic mechanism of human myosin IIIA. J Biol Chem 2007;282:216–231.
44. Muller RT, Honnert U, Reinhard J, Bahler M. The rat myosin myr 5 is a GTPase-activating protein for Rho in vivo: essential role of arginine 1695. Mol Biol Cell 1997;8:2039–2053.
45. Post PL, Bokoch GM, Mooseker MS. Human myosin-IXb is a mechanochemically active motor and a GAP for rho. J Cell Sci 1998;111(Pt 7):941–950.
46. Kong R, Yi F, Wen P, Liu J, Chen X, Ren J, Li X, Shang Y, Nie Y, Wu K, Fan D, Zhu L, Feng W, Wu JY. Myo9b is a key player in SLIT/ROBO-mediated lung tumor suppression. J Clin Invest 2015;125:4407–4420.
47. Loubery S, Coudrier E. Myosins in the secretory pathway: tethers or transporters? Cell Mol Life Sci 2008;65:2790–2800.
48. Lister I, Schmitz S, Walker M, Trinick J, Buss F, Veigel C, Kendrick-Jones J. A monomeric myosin VI with a large working stroke. EMBO J 2004;23:1729–1738.
49. Park H, Ramamurthy B, Travaglia M, Safer D, Chen LQ, Franzini-Armstrong C, Selvin PR, Sweeney HL. Full-length myosin VI dimerizes and moves processively along actin filaments upon monomer clustering. Mol Cell 2006;21:331–336.
50. Spudich G, Chibalina MV, Au JS, Arden SD, Buss F, Kendrick-Jones J. Myosin VI targeting to clathrin-coated structures and dimerization is mediated by binding to Disabled-2 and PtdIns(4,5)P2. Nat Cell Biol 2007;9:176–183.
51. Phichith D, Travaglia M, Yang Z, Liu X, Zong AB, Safer D, Sweeney HL. Cargo binding induces dimerization of myosin VI. Proc Natl Acad Sci USA 2009;106:17320–17324.
52. Yu C, Feng W, Wei ZY, Miyanoiri Y, Wen WY, Zhao YX, et al. Myosin VI undergoes cargo-mediated dimerization. Cell 2009;138:537–548.
53. Iwaki M, Tanaka H, Iwane AH, Katayama E, Ikebe M, Yanagida T. Cargo-binding makes a wild-type single-headed myosin-VI move processively. Biophys J 2006;90:3643–3652.
54. Wells AL, Lin AW, Chen LQ, Safer D, Cain SM, Hasson T, Carragher BO, Milligan RA, Sweeney HL. Myosin VI is an actin-based motor that moves backwards. Nature 1999;401:505–508.
55. Sweeney HL, Houdusse A. Myosin VI rewrites the rules for myosin motors. Cell 2010;141:573–582.
56. Morris SM, Cooper JA. Disabled-2 colocalizes with the LDLR in clathrin-coated pits and interacts with AP-2. Traffic 2001;2:111–123.
57. Sahlender DA, Roberts RC, Arden SD, Spudich G, Taylor MJ, Luzio JP, Kendrick-Jones J, Buss F. Optineurin links myosin VI to the Golgi complex and is involved in Golgi organization and exocytosis. J Cell Biol 2005;169:285–295.
58. Liu Y, Hsin J, Kim H, Selvin PR, Schulten K. Extension of a three-helix bundle domain of myosin VI and key role of calmodulins. Biophys J 2011;100:2964–2973.
59. Mukherjea M, Ali MY, Kikuti C, Safer D, Yang Z, Sirkia H, Ropars V, Houdusse A, Warshaw DM, Sweeney HL. Myosin VI must dimerize and deploy its unusual lever arm in order to perform its cellular roles. Cell Rep 2014;8:1522–1532.
60. Rock RS, Rice SE, Wells AL, Purcell TJ, Spudich JA, Sweeney HL. Myosin VI is a processive motor with a large step size. Proc Natl Acad Sci USA 2001;98:13655–13659.
61. Reed BC, Cefalu C, Bellaire BH, Cardelli JA, Louis T, Salamon J, Bloecher MA, Bunn RC. GLUT1CBP(TIP2/GIPC1) interactions with GLUT1 and myosin VI: evidence supporting an adapter function for GLUTICBP. Mol Biol Cell 2005;16:4183–4201.
62. Chibalina MV, Seaman MN, Miller CC, Kendrick-Jones J, Buss F. Myosin VI and its interacting protein LMTK2 regulate tubule formation and transport to the endocytic recycling compartment. J Cell Sci 2007;120(Pt 24):4278–4288.
63. Sakai T, Umeki N, Ikebe R, Ikebe M. Cargo binding activates myosin VIIA motor function in cells. Proc Natl Acad Sci USA 2011;108:7028–7033.
64. Bookwalter CS, Lord M, Trybus KM. Essential features of the class V myosin from budding yeast for ASH1 mRNA transport. Mol Biol Cell 2009;20:3414–3421.
65. Shi H, Singh N, Esselborn F, Blobel G. Structure of a myosin center dot adaptor complex and pairing by cargo. Proc Natl Acad Sci USA 2014;111:E1082–E1090.
66. Stoffler HE, Bahler M. The ATPase activity of Myr3, a rat myosin I, is allosterically inhibited by its own tail domain and by Ca^{2+} binding to its light chain calmodulin. J Biol Chem 1998;273:14605–14611.
67. Krementsov DN, Krementsova EB, Trybus KM. Myosin V: regulation by calcium, calmodulin, and the tail domain. J Cell Biol 2004;164:877–886.
68. Li XD, Mabuchi K, Ikebe R, Ikebe M. Ca^{2+}-induced activation of ATPase activity of myosin Va is accompanied with a large conformational change. Biochem Biophys Res Commun 2004;315:538–545.
69. Wang F, Thirumurugan K, Stafford WF, Hammer JA III, Knight PJ, Sellers JR. Regulated conformation of myosin V. J Biol Chem 2004;279:2333–2336.
70. Umeki N, Jung HS, Watanabe S, Sakai T, Li XD, Ikebe R, Craig R, Ikebe M. The tail binds to the head-neck domain, inhibiting ATPase activity of myosin VIIA. Proc Natl Acad Sci USA 2009;106:8483–8488.
71. Yang Y, Baboolal TG, Siththanandan V, Chen M, Walker ML, Knight PJ, Peckham M, Sellers JR. A FERM domain autoregulates *Drosophila* myosin 7a activity. Proc Natl Acad Sci USA 2009;106:4189–4194.
72. Umeki N, Jung HS, Sakai T, Sato O, Ikebe R, Ikebe M. Phospholipid-dependent regulation of the motor activity of myosin X. Nat Struct Mol Biol 2011;18:783–788.
73. Wei ZY, Liu XT, Yu C, Zhang MJ. Structural basis of cargo recognitions for class V myosins. Proc Natl Acad Sci USA 2013;110:11314–11319.
74. Li XD, Jung HS, Wang Q, Ikebe R, Craig R, Ikebe M. The globular tail domain puts on the brake to stop the ATPase cycle of myosin Va. Proc Natl Acad Sci USA 2008;105:1140–1145.

75. Li XD, Ikebe R, Ikebe M. Activation of myosin Va function by melanophilin, a specific docking partner of myosin Va. J Biol Chem 2005;280:17815–17822.
76. Fukuda M, Kuroda TS, Mikoshiba K. Slac2-a/melanophilin, the missing link between Rab27 and myosin Va: implications of a tripartite protein complex for melanosome transport. J Biol Chem 2002;277:12432–12436.
77. Strom M, Hume AN, Tarafder AK, Barkagianni E, Seabra MC. A family of Rab27-binding proteins. Melanophilin links Rab27a and myosin Va function in melanosome transport. J Biol Chem 2002;277:25423–25430.
78. Kukimoto-Niino M, Sakamoto A, Kanno E, Hanawa-Suetsugu K, Terada T, Shirouzu M, Fukuda M, Yokoyama S. Structural basis for the exclusive specificity of Slac2-a/melanophilin for the Rab27 GTPases. Structure 2008;16:1478–1490.
79. Mercer JA, Seperack PK, Strobel MC, Copeland NG, Jenkins NA. Novel myosin heavy chain encoded by murine dilute coat colour locus. Nature 1991;349:709–713.
80. Sckolnick M, Krementsova EB, Warshaw DM, Trybus KM. More than just a cargo adapter, melanophilin prolongs and slows processive runs of myosin Va. J Biol Chem 2013;288:29313–29322.
81. Pylypenko O, Attanda W, Gauquelin C, Lahmani M, Coulibaly D, Baron B, Hoos S, Titus MA, England P, Houdusse AM. Structural basis of myosin V Rab GTPase-dependent cargo recognition. Proc Natl Acad Sci USA 2013;110:20443–20448.
82. Yao LL, Cao QJ, Zhang HM, Zhang J, Cao Y, Li XD. Melanophilin stimulates myosin-5a motor function by allosterically inhibiting the interaction between the head and tail of myosin-5a. Sci Rep 2015;5:10874.
83. Wu XS, Rao K, Zhang H, Wang F, Sellers JR, Matesic LE, Copeland NG, Jenkins NA, Hammer JA III. Identification of an organelle receptor for myosin-Va. Nat Cell Biol 2002;4:271–278.
84. Ji HH, Zhang HM, Shen M, Yao LL, Li XD. The motor function of *Drosophila melanogaster* myosin-5 is activated by calcium and cargo-binding protein dRab11. Biochem J 2015;469:135–144.
85. Sakai T, Jung HS, Sato O, Yamada MD, You DJ, Ikebe R, Ikebe M. Structure and regulation of the movement of human myosin VIIA. J Biol Chem 2015;290:17587–17598.
86. Odronitz F, Kollmar M. Drawing the tree of eukaryotic life based on the analysis of 2,269 manually annotated myosins from 328 species. Genome Biol 2007;8:R196.
87. Hales CM, Vaerman JP, Goldenring JR. Rab11 family interacting protein 2 associates with myosin Vb and regulates plasma membrane recycling. J Biol Chem 2002;277:50415–50421.
88. Chen XW, Leto D, Chiang SH, Wang Q, Saltiel AR. Activation of RalA is required for insulin-stimulated Glut4 trafficking to the plasma membrane via the exocyst and the motor protein Myo1c. Dev Cell 2007;13:391–404.
89. Grati M, Kachar B. Myosin VIIa and sans localization at stereocilia upper tip-link density implicates these Usher syndrome proteins in mechanotransduction. Proc Natl Acad Sci USA 2011;108: 11476–11481.
90. Wu L, Pan LF, Wei ZY, Zhang MJ. Structure of MyTH4-FERM domains in myosin VIIa tail bound to cargo. Science 2011;331:757–760.
91. Pan LF, Zhang MJ. Structures of usher syndrome 1 proteins and their complexes. Physiology 2012;27:25–42.
92. Kussel-Andermann P, El-Amraoui A, Safieddine S, Nouaille S, Perfettini I, Lecuit M, Cossart P, Wolfrum U, Petit C. Vezatin, a novel transmembrane protein, bridges myosin VIIA to the cadherin-catenins complex. EMBO J 2000;19:6020–6029.
93. Etournay R, Zwaenepoel I, Perfettini I, Legrain P, Petit C, El-Amraoui A. Shroom2, a myosin-VIIa- and actin-binding protein, directly interacts with ZO-1 at tight junctions. J Cell Sci 2007;120(Pt 16): 2838–2850.
94. Senften M, Schwander M, Kazmierczak P, Lillo C, Shin JB, Hasson T, Geleoc GS, Gillespie PG, Williams D, Holt JR, Muller U. Physical and functional interaction between protocadherin 15 and myosin VIIa in mechanosensory hair cells. J Neurosci 2006;26:2060–2071.
95. Kerber ML, Cheney RE. Myosin-X: a MyTH-FERM myosin at the tips of filopodia. J Cell Sci 2011;124(Pt 22):3733–3741.
96. Courson DS, Cheney RE. Myosin-X and disease. Exp Cell Res 2015;334:10–15.
97. Lu Q, Yu J, Yan J, Wei ZY, Zhang MJ. Structural basis of the myosin X PH1(N)-PH2-PH1(C) tandem as a specific and acute cellular PI(3,4,5)P-3 sensor. Mol Biol Cell 2011;22:4268–4278.
98. Hirano Y, Hatano T, Takahashi A, Toriyama M, Inagaki N, Hakoshima T. Structural basis of cargo recognition by the myosin-X MyTH4-FERM domain. EMBO J 2011;30:2734–2747.
99. Wei Z, Yan J, Lu Q, Pan L, Zhang M. Cargo recognition mechanism of myosin X revealed by the structure of its tail MyTH4-FERM tandem in complex with the DCC P3 domain. Proc Natl Acad Sci USA 2011;108:3572–3577.
100. Xie X, Harrison DH, Schlichting I, Sweet RM, Kalabokis VN, Szent-Gyorgyi AG, Cohen C. Structure of the regulatory domain of scallop myosin at 2.8 A resolution. Nature 1994;368:306–312.
101. Houdusse A, Cohen C. Structure of the regulatory domain of scallop myosin at 2 A resolution: implications for regulation. Structure 1996; 4:21–32.
102. Heissler SM, Sellers JR. Myosin light chains: teaching old dogs new tricks. Bioarchitecture 2014;4:169–188.
103. Zhu T, Sata M, Ikebe M. Functional expression of mammalian myosin I beta: analysis of its motor activity. Biochemistry 1996;35: 513–522.
104. Manceva S, Lin TM, Pham H, Lewis JH, Goldman YE, Ostap EM. Calcium regulation of calmodulin binding to and dissociation from the myo1c regulatory domain. Biochemistry 2007;46:11718–11726.
105. Lieto-Trivedi A, Coluccio LM. Calcium, nucleotide, and actin affect the interaction of mammalian Myo1c with its light chain calmodulin. Biochemistry 2008;47:10218–10226.
106. Munnich S, Taft MH, Manstein DJ. Crystal structure of human myosin 1c – the motor in GLUT4 exocytosis: implications for Ca2+ regulation and 14-3-3 binding. J Mol Biol 2014;426:2070–2081.
107. Shuman H, Greenberg MJ, Zwolak A, Lin T, Sindelar CV, Dominguez R, Ostap EM. A vertebrate myosin-I structure reveals

unique insights into myosin mechanochemical tuning. Proc Natl Acad Sci USA 2014;111:2116–2121.
108. Lu Z, Shen M, Cao Y, Zhang HM, Yao LL, Li XD. Calmodulin bound to the first IQ motif is responsible for calcium-dependent regulation of myosin 5a. J Biol Chem 2012;287:16530–16540.
109. Rzadzinska AK, Nevalainen EM, Prosser HM, Lappalainen P, Steel KP. MyosinVIIa interacts with Twinfilin-2 at the tips of mechanosensory stereocilia in the inner ear. PLoS One 2009;4:e7097.
110. Salles FT, Merritt RC Jr, Manor U, Dougherty GW, Sousa AD, Moore JE, Yengo CM, Dose AC, Kachar B. Myosin IIIa boosts elongation of stereocilia by transporting espin 1 to the plus ends of actin filaments. Nat Cell Biol 2009;11:443–450.
111. Manor U, Disanza A, Grati M, Andrade L, Lin H, Di Fiore PP, Scita G, Kachar B. Regulation of stereocilia length by myosin XVa and whirlin depends on the actin-regulatory protein Eps8. Curr Biol 2011;21: 167–172.
112. Merritt RC, Manor U, Salles FT, Grati M, Dose AC, Unrath WC, Quintero OA, Yengo CM, Kachar B. Myosin IIIB uses an actin-binding motif in its espin-1 cargo to reach the tips of actin protrusions. Curr Biol 2012;22:320–325.
113. Liu H, Li J, Raval MH, Yao N, Deng X, Lu Q, Nie S, Feng W, Wan J, Yengo CM, Liu W, Zhang M. Myosin III-mediated cross-linking and stimulation of actin bundling activity of Espin. Elife 2016;5:e12856.